

## Geometry and time scale of the rotational dynamics in supercooled toluene

G. Hinze

*Institut für Physikalische Chemie, Johannes Gutenberg-Universität, 55099 Mainz, Germany*

(Received 12 September 1997)

Multidimensional deuteron NMR provides powerful tools for studying molecular reorientation in supercooled liquids. We present results on selectively deuterated toluene- $d_5$ , which may be one of the molecularly most simple van der Waals glass formers. From two-time correlation functions the time scale of reorientation was obtained slightly above the calorimetric glass transition temperature. The applied stimulated echo method provides a geometry parameter that, in analogy to  $q$ -dependent scattering experiments, allows one to investigate the geometry of the elementary rotational process. Continuous time random walk computer simulations were used for the interpretation of the data. It is shown that an isotropic single jump angle model does not describe the toluene rotation, rather the existence of several jump angles is required. Assuming mainly small jump angles  $< 6^\circ$  but also some larger angles up to  $30^\circ$  an acceptable fit to the experimental data was obtained. Using four-time correlation functions further properties of molecular reorientation are elucidated. Slow reorienting subensembles can be selected. Their return to the full ensemble occurs on the same time scale as the elementary rotational jump process. In accord with previous investigations in other supercooled liquids, a heterogeneous scenario is found for the rotational dynamics of toluene. [S1063-651X(98)10402-6]

PACS number(s): 61.20.Lc, 61.25.-f, 61.43.Fs, 64.70.Pf

### I. INTRODUCTION

One prominent feature of glass forming liquids is the slowing down of the characteristic time scale associated with structural relaxation over many decades with decreasing temperature. Although this behavior is found qualitatively with many experimental methods, there are indications for slight differences for different observables. In several supercooled liquids, e.g., a so-called temperature dependent decoupling of translational and rotational dynamics occurs [1]. Here, different properties are compared, but even the rotational dynamics alone as observed with two different methods leads to different results. A recent comparison of dielectric relaxation and relaxation times from NMR of supercooled toluene near the calorimetric glass transition indicates deviations that cannot be explained by the different Legendre polynomials associated with the two methods [2]. Most recently, several of these apparent differences including the translational-rotational decoupling have been interpreted within a simple energy landscape model [3,4]. In this model, transitions between different energy minima are directly connected with rotational and translational dynamics. It turns out that for a quantitative description of experimental data by this model the geometry of the molecular dynamics is essential.

Mode coupling theory (MCT) describes density fluctuations and predicts a variety of time scales on which dynamics occurs [5]. In a recent extension of this theory to molecular liquids orientational degrees of freedom were included in addition to density fluctuations [6]. It was found that by this extension different strengths of the  $\alpha$  peak with respect to the microscopic peak are possible, depending on whether dielectric relaxation or density fluctuations are considered. With regard to the MCT extension it becomes necessary to study the rotational dynamics of supercooled liquids in more detail in order to understand certain differences in the  $\alpha$ -peak scenario, which are experimentally well known [7].

Another characteristic of supercooled liquids near  $T_g$  is

seen in the pronounced non-Debye spectral density observed, e.g., in dielectric experiments. Controversial discussions concerning the origin of the nonexponential  $\alpha$  relaxation led to a number of experiments dealing with this question. In principle two extreme scenarios are conceivable. In the *homogeneous* picture all molecules of a sample relax in a similar but nonexponential way. The other extreme is the *heterogeneous* case, where a distribution of exponential relaxations leads to the nonexponentiality. Several recently developed experimental techniques allow for studying this issue [8,9,10]. The underlying principle of these experiments is roughly the same. First a dynamically distinguishable subensemble is selected and then its relaxation back to the overall dynamics is observed. In that way a nonhomogeneous scenario was found in several glass forming liquids and polymers [8–13]. Furthermore, there are indications for dynamical exchange, which means that, e.g., slowly reorienting molecules become fast and vice versa.

Altogether it turns out that the detailed knowledge of the dynamics in supercooled liquids is essential for an understanding of the vitrification process. Therefore there is much interest in the study of glass forming liquids consisting of simple molecules. One of the molecularly most simple van der Waals bonded glass formers may be supercooled toluene ( $C_6H_5-CH_3$ ). Of course the methyl group attached to the phenyl ring performs rapid rotations around its  $C_3$  axis. On the other hand at temperatures near  $T_g$  and above, this internal motion is fast compared to the overall structural relaxation. Therefore only a time-averaged molecular structure needs to be considered. Detailed studies on the methyl-group rotation in the glassy state of toluene were performed [14] and will be published elsewhere.

In this work phenyl-ring deuterated toluene has been measured slightly above  $T_g$  using deuteron NMR. The main advantage of  $^2H$ -NMR is that it provides a means to measure single particle correlation functions. On the other hand selectively deuterated compounds allow one to focus on the de-

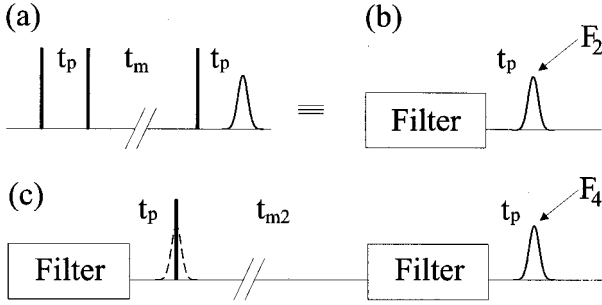


FIG. 1. The stimulated echo sequence (a) can be understood as a dynamical filter (b) allowing only slow reorienting molecules to pass. The reduced 4D NMR experiment (c) now consists of two successive  $F_2$  pulse sequences.  $t_p$  and  $t_m$  determine the filter function, only  $t_{m2}$  is varied leading to  $F_4(t_{m2})$ .

sired dynamics. In the case of toluene- $d_5$  the phenyl-ring rotation becomes observable. Stimulated echo techniques were applied in order to obtain insight into the different aspects of the rotational dynamics. Along with the determination of rotational correlation times as a function of temperature a detailed analysis of the elementary molecular rotation process is performed. Using four-time stimulated echo experiments the dynamical heterogeneity of the reorientation is studied.

The remainder of the paper is organized as follows. In the next section we present the experimental methods to measure the different two- and four-time rotational correlation functions. The experimental results are discussed in Sec. III and we close with some conclusions in Sec. IV.

## II. EXPERIMENTAL DETAILS

### A. Two-time correlation functions

In deuteron NMR the molecular orientation  $\Omega$  is probed directly via the angular dependence of the quadrupolar frequency  $\omega(\theta) = \pm \delta P_2(\cos \theta)$ . The angle enclosed by the direction of a C-D bond and the external magnetic field is denoted by  $\theta$ , the quadrupolar coupling constant for toluene- $d_5$  is  $\delta = (1.18 \mu\text{s})^{-1}$  [15]. By applying a standard three pulse sequence [see Fig. 1(a)] [16], two-time rotational correlation functions can be measured. Here the orientation dependent quadrupolar frequencies are correlated before and after a mixing time  $t_m$ . With appropriately chosen pulse phases two different functions,

$$F_2^{ss} = \langle \sin[\omega(0)t_p] \sin[\omega(t_m)t_p] \rangle / \langle \sin^2[\omega(0)t_p] \rangle \quad (1)$$

and

$$F_2^{cc} = \langle \cos[\omega(0)t_p] \cos[\omega(t_m)t_p] \rangle / \langle \cos^2[\omega(0)t_p] \rangle \quad (2)$$

can be obtained.  $t_p$  is the evolution time and adjusts the sensitivity of the experiment with respect to changes in the quadrupolar frequencies.

For our first application  $F_2^{ss}$  is considered in the limit  $t_p \rightarrow 0$  where Eq. (1) becomes the autocorrelation function of the Legendre polynomial  $P_2(\cos[\theta])$  [1]

$$F_2^{ss}(t_p \rightarrow 0, t_m) = \langle P_2(\cos[\theta(0)]) P_2(\cos[\theta(t_m)]) \rangle. \quad (3)$$

Under the assumption of isotropic reorientation the mean rotational correlation time is now defined by

$$\langle \tau_c \rangle = \int_0^\infty F_2^{ss}(t_p \rightarrow 0, t_m) dt_m. \quad (4)$$

In this work the rotational isotropy was not explicitly demonstrated, but it is found in similar supercooled molecular liquids like *o*-terphenyl (OTP) [22] or glycerol [17].

A restriction of the time window accessible to the stimulated echo method is given in principal by spin-spin and spin-lattice relaxation. In addition to decorrelation due to molecular reorientation, both effects lead to loss of magnetization. Since spin-spin relaxation acts only during the evolution period, it is negligible in the limit  $t_p \rightarrow 0$ . Spin-lattice relaxation on the other hand becomes important during the mixing time and can therefore mask the desired rotational correlation function. Therefore a separate measurement of the spin-lattice relaxation is advisable. In the case of  $F_2^{cc}$  the spin-lattice relaxation of the Zeeman order ( $T_1$ ) can easily be measured by standard techniques. This is the reason why we used these correlation functions to learn about the rotational geometry. The situation is somewhat more complicated in the case of  $F_2^{ss}$ , where spin-lattice relaxation of quadrupolar order ( $T_{1Q}$ ) becomes important. This contribution cannot be measured independently from the rotational correlation function.

Virtually all experimental methods for studying molecular reorientations measure rotational correlation times, depending on the elementary rotational jump process. The correlation functions  $F_2^{ss}(t_p \rightarrow 0, t)$  decay to  $1/e$ , if the molecules have reoriented around a particular angle, which for  $L=2$  methods is between  $42^\circ$  and  $57^\circ$ . On the other hand, at the same time their *jump* correlation functions [18] can differ enormously. In the following we consider an isotropic jump process with a constant jump angle  $\Delta\theta$ . Then the jump correlation time  $\tau_j$  is related to the rotational correlation time  $\tau_c$  by [18]

$$\frac{\tau_j}{\tau_c} = \frac{3}{2} \sin^2 \Delta\theta. \quad (5)$$

Similar relations hold for the correlation times as extracted from methods such as, e.g., dielectric spectroscopy ( $L=1$ ). In the limit of infinitesimally small angles  $\Delta\theta \rightarrow 0$  the standard rotational diffusion model is obtained and  $\tau_j$  is no longer defined. The other extreme is the rotational random jump scenario, where both correlation times  $\tau_j$  and  $\tau_c$  are equal.

The stimulated echo method now provides the possibility to measure both correlation times depending on the chosen evolution time  $t_p$ . In the limit  $t_p \rightarrow 0$  one obtains  $\tau_c$ , while for very large  $t_p$  (depending on the jump angle) the elementary jump correlation time  $\tau_j$  is accessible. In addition, correlation times  $\tau(t_p)$  corresponding to the intermediate  $t_p$  regime provide further information on the rotational geometry. The analogy to a scattering experiment is straightforward. While at small scattering vector  $q$  (small  $t_p$ ) long-time diffusion can be observed, at large enough scattering vectors  $q$  elementary jump processes are seen [19].

We have measured the detailed  $t_p$  dependence of the correlation functions  $F_2^{cc}(t_p, t_m)$  to investigate geometric aspects of molecular rotation. In principle the same information can be obtained from  $F_2^{ss}(t_p, t_m)$ , which, however, can be affected by  $T_{1Q}$ , as discussed above. The larger the evolution time  $t_p$  is chosen, the smaller the changes in the quadrupolar frequency  $\omega$  are that can be resolved. Correspondingly, in this limit reorientations by relatively small angles lead to a decay of  $F_2^{cc}$  already. With a whole set of  $t_p$  dependent correlation functions the geometry of the elementary rotational process can be analyzed in detail. Interpreting  $t_p$  as a “generalized” scattering vector  $q$  nothing but a  $q$  dependent “scattering experiment” is carried out [20]. The well known deuteron 2D NMR exchange spectroscopy represents a similar experiment in the frequency domain [21]. Especially in systems where molecules reorient via large angular jumps this method allows for data interpretation without any model assumptions. However, the time domain analysis of the stimulated echo as carried out in this paper provides a higher resolution on small angle jumps [22,23].

### B. Four-time correlation functions

Since a detailed description of the reduced 4D NMR experiment is given elsewhere [8,11,13,24], the basic idea of this method is only sketched here. Combining Eqs. (1) and (2) one obtains  $F_2 \equiv (F_2^{ss} + F_2^{cc})/2 = \langle \cos[\omega(0) - \omega(t_m)] t_p \rangle$ . Assuming a rotational jump process, for large evolution times  $\delta t_p \gg 1$  this function can be understood as a *dynamical* filter of molecular reorientation (see Fig. 1). Any rotational jump that takes place during  $t_m$  alters the NMR frequency of a molecule to such an extent that its contribution to  $F_2$  vanishes. Only the fraction of molecules that have not jumped during the mixing time  $t_m$  contribute to  $F_2$ . In this picture no enhanced return-jump probability [25] is assumed as it is justified, e.g., in the case of the rotational random jump model.

The reduced 4D NMR experiment now consists of two successive  $F_2$  pulse sequences. With the first one, a subensemble of molecules is selected, which have not reoriented during the first mixing time  $t_{m1}$ . Their magnetization is stored with an additional pulse. After a mixing time  $t_{m2}$ , the second  $F_2$  sequence is applied with the same parameters as the first one. Therewith the same filter is applied twice. Only slow molecules, which pass the first filter and remain slow during  $t_{m2}$ , will also pass the second filter and contribute to the four-time correlation function

$$E_4(t_{m2}) = \langle \cos[(\omega_1 - \omega_2)t_p] \cos[(\omega_3 - \omega_4)t_p] \rangle, \quad (6)$$

with  $\omega_1 = \omega(t=0)$ ,  $\omega_2 = \omega(t=t_m)$ ,  $\omega_3 = \omega(t=t_m + t_{m2})$ , and  $\omega_4 = \omega(t=2t_m + t_{m2})$ . On the other hand, slow molecules that become fast during  $t_{m2}$  cannot pass the second filter and therefore lead to an attenuation of  $E_4(t_{m2})$ . From these considerations, the normalized function  $F_4(t_{m2}) = E_4(t_{m2})/E_4(0)$  can be seen as a correlation function for dynamical exchange. Indeed, under ideal conditions the correlation function  $F_4(t_{m2})$  does not depend on the jump process and reflects only dynamical changes. In the case of small jump angles, on the other hand, if the condition  $\Delta\theta > \pi(t_p\delta)^{-1}$  is no longer fulfilled, contributions from the ro-

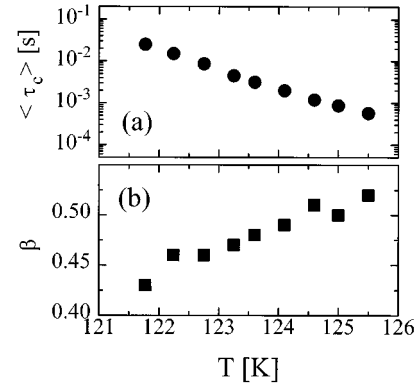


FIG. 2. (a) Mean *rotational* correlation times of toluene- $d_5$  obtained with the stimulated echo technique. (b) The stretching exponents  $\beta$  of the corresponding correlation functions decrease with decreasing temperature.

tation are also seen in  $F_4$  as was experimentally demonstrated for the case of rotational diffusion of polymer colloids [26]. From this observation it becomes obvious that the knowledge of the elementary rotational jump geometry is required for interpreting four-time correlation functions.

### C. Experimental setup

All experiments discussed in this paper have been performed on a home built spectrometer at a  $^2\text{H}$  Larmor frequency of 40.2 MHz with a typical  $\pi/2$  pulse length of 2.8  $\mu\text{s}$ . Temperature stability to within  $\pm 0.1$  K was maintained using a static flow cryostat from Oxford Instruments.

## III. RESULTS AND DISCUSSION

### A. Rotational time scales

Rotational correlation times  $\langle \tau_c \rangle$  of toluene- $d_5$  have been measured in the temperature range 121.7–125.5 K slightly above the calorimetric glass transition temperature  $T_g = 117.5$  K [27]. In comparison to earlier measurements [15], the accessible regime of correlation times could be enlarged by a factor of four using an extended phase cycle [26]. It should be noted that temperature stability and accuracy were examined carefully, since already small deviations lead to enormous variations in correlation times. In the entire temperature regime nonexponential correlation functions were found that could be fitted to the stretched exponential function  $F_2^{ss} \propto \exp[-(t/\tau_c)^\beta]$ . A mean correlation time was obtained by integrating the normalized  $F_2^{ss}$  [cf. Eq. (4)] leading to  $\langle \tau_c \rangle = \tau_c \beta^{-1} \Gamma(\beta^{-1})$ , where  $\Gamma$  denotes the gamma function. In Fig. 2(a) the rotational correlation times of toluene thus determined are plotted versus temperature. From recent dielectric relaxation measurements [2] it was found that toluene shows a very fragile behavior. There a fragility index  $m = 105$  was obtained by analyzing the temperature dependence around  $T_g$  [28]. It turns out that toluene is one of the most fragile aromatic low-molecular-weight liquids. However, the above-mentioned dielectric relaxation times are a factor of ten shorter in this regime, which could not be explained by the fact that the different techniques yield different mean values or the different order of the Legendre polynomials [2].

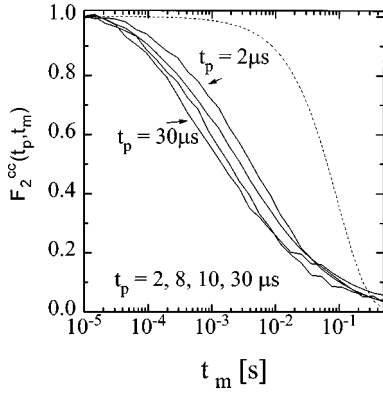


FIG. 3. Toluene- $d_5$  rotational correlation functions  $F_2^{cc}(t_p, t_m)$  for different evolution times  $t_p$ , measured at  $T=122.2$  K. The decay of the longitudinal magnetization (dashed line) is well separated from the rotational correlation functions.

Not only the distinct temperature dependence of the structural relaxation but also the pronounced nonexponentiality of the corresponding correlation functions is a characteristic of supercooled liquids near  $T_g$ . In toluene we find a stretching parameter of  $\beta \approx 0.5$  for the rotational correlation function. The slight temperature dependence of  $\beta$  is plotted in Fig. 2(b). With decreasing temperatures the correlation functions  $F_2^{ss}$  become more nonexponential. It should be noted that qualitatively the same tendency was found in the width of the spectral densities obtained by dielectric spectroscopy [29]. In Sec. III C of this paper we will focus on further details of this non-Debye behavior.

The influence of the spin-lattice relaxation  $T_{1Q}$  on the obtained correlation functions was estimated as follows. From other glass formers such as *o*-terphenyl and glycerol it is known that at temperatures around  $T_g$  the quadrupolar order decay time  $T_{1Q}$  decays about 6–8 times faster than the Zeeman order  $T_1$ . Therefore it is expected that only at the lowest temperature measured here (121.7 K,  $\langle T_1 \rangle \approx 0.2$  s) the rotational correlation time of toluene ( $\langle \tau_c \rangle = 0.025$  s) could be affected by  $T_{1Q}$ . At higher temperatures the time scales of spin-lattice relaxation and reorientation become more and more different, so that  $T_{1Q}$  effects can be neglected.

### B. Rotational geometry

With a detailed set of  $t_p$  dependent correlation functions  $F_2^{cc}(t_p, t_m)$  geometric aspects of molecular reorientation are accessible. Since the measurements are relatively time consuming, data were measured only at one temperature  $T = 122.2$  K. The spin-lattice relaxation time  $T_1$  was determined separately. We found an almost exponential magnetization decay, which could be fitted with  $\exp[-(t/0.097s)^{0.94}]$ . The rotational correlation time  $\langle \tau_c \rangle = 0.023$  s was measured as described in the previous section.

The obtained  $F_2^{cc}$  data are analyzed following Geil *et al.* [22]. In a first step we parametrize the experimental data (see Fig. 3) with a stretched exponential function  $\exp\{-[t/\tau(t_p)]^{\beta(t_p)}\}$  to obtain the time scales  $\tau(t_p)$  and the widths  $\beta(t_p)$  of the correlation functions. It turns out that the two parameters  $\tau(t_p)$  and  $\beta(t_p)$  reflect two different aspects of the reorientation, at least if the distribution of rotational

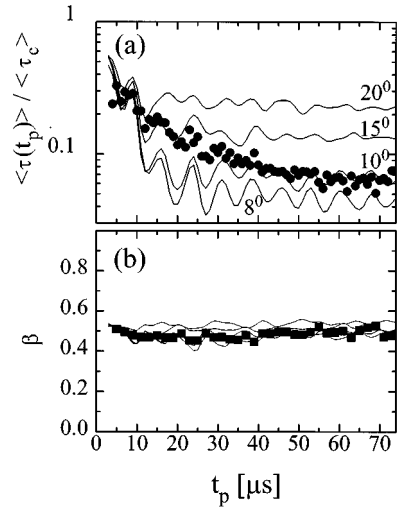


FIG. 4. Results from the parametrization of the  $F_2^{cc}$  correlation functions. (a) For larger evolution times  $t_p > 50 \mu\text{s}$  the experimental mean correlation times  $\langle \tau(t_p) \rangle$  (●) reach a plateau value that is compatible with a simple rotational jump model that assumes one distinct jump angle  $10^\circ$  and a static distribution of correlation times. (b) The width parameter  $\beta$  shows no significant  $t_p$  dependence.

correlation times is very broad as it is in the case of toluene- $d_5$ . Then  $\beta(t_p)$  is dominated by the width of the distribution, whereas the geometry of reorientation is comprised of  $\tau(t_p)$ .

In Fig. 4 the resulting  $\langle \tau(t_p) \rangle / \langle \tau_c \rangle$  [full circles, Fig. 4(a)] and  $\beta(t_p)$  [full squares, Fig. 4(b)] data of the  $t_p$  dependent correlation functions are plotted for one temperature. The mean correlation times were calculated from the fit parameters again by  $\langle \tau(t_p) \rangle = \tau(t_p) \beta^{-1} \Gamma(\beta^{-1})$ . To simplify the representation, in the following only relative time scales  $\langle \tau(t_p) \rangle / \langle \tau_c \rangle$  are considered. The oscillations of  $\langle \tau(t_p) \rangle$  as a function of  $t_p$  are due to the cosine functions in  $F_2^{cc}$  [Eq. (2)] and would be phase shifted considering  $F_2^{ss}$ . However, as seen in Fig. 4(b), the width parameters  $\beta$  are about 0.5 and show no significant  $t_p$  dependence. Neglecting the oscillations in Fig. 4(a), the mean correlation times  $\langle \tau(t_p) \rangle$  decrease with increasing  $t_p$  and become almost constant for  $t_p > 50 \mu\text{s}$ . At these evolution times we are in the limit of measuring the jump correlation time  $\langle \tau_j \rangle$ . Applying Eq. (5) to the plateau value, a mean jump angle of  $\Delta\theta \approx 11^\circ$  can be estimated. It is noted that this rough estimate does not take into account either a distribution of correlation times or a distribution of jump angles.

To analyze the rotational geometry in more detail, we have compared the experimental data with model calculations. For this purpose we have used several isotropic rotational jump models. Starting from a randomly chosen orientation, molecular reorientation is modeled to consist of rotational jumps with well defined jump angles  $\Delta\theta$ . In the limit of  $\Delta\theta \rightarrow 0$  the standard rotational diffusion model is obtained. A detailed description of the model calculations is given in Appendix A.

In our first simulation a rotational jump model was assumed that incorporated fixed jump angles and a log-Gauss distribution of correlation times. The width of the distribution was chosen to fit the  $\beta(t_p)$  values in Fig. 4(b). To illustrate the effect of different jump angles on  $\langle \tau(t_p) \rangle$ , in Fig.

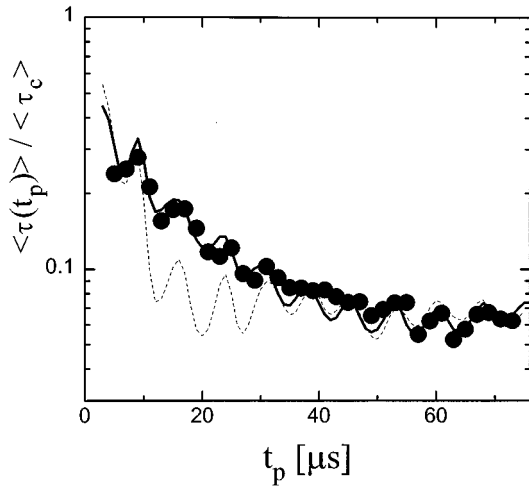


FIG. 5. The experimental data (●) are the same as in Fig. 4. The solid line represents the simulation with two rotational jump angles 80% 4° and 20% 25°. The simplest model with only one jump angle deviates significantly in the intermediate regime  $1 \mu\text{s} < t_p < 30 \mu\text{s}$  (dashed line).

4(a) the calculated data are plotted (full lines) for several fixed jump angles. With increasing  $t_p$  the correlation times  $\langle \tau(t_p) \rangle$  decrease and assume a plateau value for larger  $t_p$ , which depends on  $\Delta\theta$ . As mentioned above, the oscillations should be disregarded. Only in the case of rotational diffusion no constant  $\langle \tau(t_p) \rangle$  is reached for large  $t_p$ . The other limit would be the isotropic random jump model, where all correlation times  $\langle \tau(t_p) \rangle$  and  $\langle \tau_c \rangle$  are equal, but which is not considered here. From the comparison of the experimental plateau value with the single jump angle simulations [Fig. 4(a)] a mean jump angle around  $\Delta\theta \approx 10^\circ$  can be extracted. This value is somewhat smaller than our first rough estimate, since we now consider a distribution of correlation times that appears realistic. However, in the range  $2 \mu\text{s} < t_p < 20 \mu\text{s}$  significant deviations between the model calculations and the experimental data are apparent.

In addition to a distribution of correlation times, one would expect that a model with a distribution of rotational jump angles  $\Delta\theta$  gives a more realistic description of the reorientational dynamics in a supercooled liquid. Therefore, computer simulations were performed using various forms of jump angle distributions. Within the simple rotational jump simulations performed in this paper, it is straightforward to take into account such a distribution. Whenever a jump occurs, the corresponding angle  $\Delta\theta$  is chosen randomly from the given distribution.

The simplest possible distribution that we have considered consists of two components. Indeed, with mainly small jump angles and some larger ones a reasonable agreement with the data is obtained. We find an optimum with 80% 4° and 20% 25° jumps; see Fig. 5. With this choice not only the plateau but also the intermediate range  $2 \mu\text{s} < t_p < 20 \mu\text{s}$  can be described significantly better than without a distribution of jump angles. A similar picture could be obtained with, e.g., 3° and 30° jumps, but not any combination is possible. Choosing the large angle component to be 35° or larger, deviations to the experimental data become obvious. Also the deviations increase if the small angle is set below 3°. In

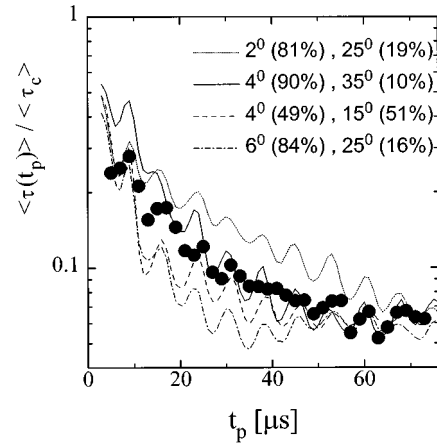


FIG. 6. Models involving four different combinations of two jump angles are simulated (lines) and compared with the experimental data (●) (see Fig. 4). Deviations from the experimental data are obvious in all calculations and demonstrate the dependence of the angle combination on the simulation result. The amount of larger and smaller angles was chosen to fit the plateau value at  $t_p = 70 \mu\text{s}$ .

Fig. 6 several combinations of jump angles are plotted to demonstrate the deviations. It should be noted that independent from the exact numerical values, mainly small jump angles are required in conjunction with a small fraction of some larger jumps in order to yield an acceptable fit to the experimental data.

An equivalent picture is obtained if continuous jump angle distributions are assumed. Many different distributions were tested, but only a few of them fit well to the experimental data. We find that symmetric distributions such as Gaussian or box distributions are incompatible with the experiment. Rather a strong asymmetry of the distribution is required. In Fig. 7(a) a truncated exponential distribution is plotted that shows similar good agreement with the data as the simple two angle model described above. This distribution again involves mainly small jump angles  $\Delta\theta$  and some larger ones.

In general two regimes of the  $t_p$  dependent correlation times can be distinguished. The first regime is characterized

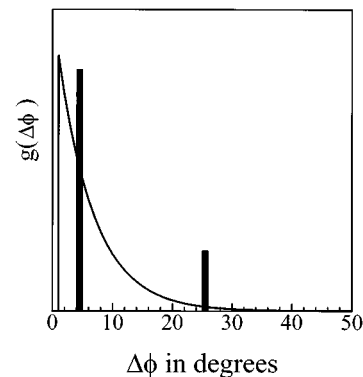


FIG. 7. Rotational jump angle distributions of the best fitting jump models. Both distributions, the continuous and the discrete distribution, are similar: in addition to mainly small rotational jumps also some larger jump angles occur. The continuous distribution is proportional to  $e^{-\Delta\theta/6^\circ}$  for  $\Delta\theta \geq 1^\circ$ .

by a decreasing of  $\langle \tau(t_p) \rangle$  with increasing  $t_p$  and in our case runs from 1  $\mu\text{s}$  to 40  $\mu\text{s}$ . As clearly demonstrated in Fig. 5, this regime yields different information on the jump geometry than the plateau regime at larger  $t_p$  values. From the first regime we learn that small angle jumps (smaller than  $10^\circ$ ) contribute significantly to the decay of the rotational correlation function. The plateau value  $\langle \tau(t_p \rightarrow \infty) \rangle$  reflects a mean jump angle. This information was also used in the data analysis of *o*-terphenyl, where a mean jump angle of  $\sim 10^\circ$  was extracted [22]. It is noted that the averaging over several jump angles is not a simple arithmetic averaging, rather it depends on the experimental methods with which the mean jump angle is observed. In our case the calculation of a mean jump angle  $\overline{\Delta\theta}$  from a distribution  $g(\Delta\theta)$  is straightforward using the plateau value given by  $\tau_j/\tau_c$  (see Appendix B):

$$\frac{\tau_j}{\tau_c} = \frac{3}{2} \int d(\Delta\theta) g(\Delta\theta) \sin^2 \Delta\theta = \frac{3}{2} \overline{\sin^2 \Delta\theta}. \quad (7)$$

It is remarkable that in a polymeric system at temperatures slightly above  $T_g$  a similar scenario with different jump angles was found [30]. Using a difference correlated exchange spectroscopy (DICO) NMR experiment, it was observed in polystyrene a rotational process with small jump angles around  $\sim 10^\circ$  but also some larger contributions of  $30^\circ$ – $40^\circ$ . The latter could not be attributed to conformational rearrangements typical for chain dynamics. In addition, from molecular dynamics simulations of a simple model of the glass former *o*-terphenyl, different types of reorientation including small angle fluctuations but also large angle jump processes were identified [31].

From our experiments we cannot determine whether small and larger angle jumps are both connected with the structural relaxation. Or should the small and large angle jumps be attributed to different dynamical processes? Although statements about this issue are speculative, it should be noted that indeed further processes faster than the structural relaxation are observable in almost every glass former. The so-called fast  $\beta$  process predicted by the MCT [5] takes place on a time scale of  $\sim 10^{-12}$  s and cannot be observed with the NMR techniques employed in this paper. On the other hand, the slow  $\beta$  process found by Johari and Goldstein [32] near  $T_g$  occurs in the kHz regime and is therefore much closer to the time window of the stimulated echo experiment. However, it is still unclear if the latter process represents an intrinsic feature of the glass transition or if it rather depends on the molecular structure. In toluene, below the glass transition a slow  $\beta$  process could be identified using NMR relaxation measurements [15], which subsequently was confirmed by dielectric measurements [29]. Due to the simple molecular structure of toluene, no intramolecular degree of freedom can be responsible for this process [33]. Rather the whole molecule undergoes some kind of librational motion, which was shown to be highly anisotropic [34]. In supercooled *o*-terphenyl it was found in dielectric experiments that the slow  $\beta$  process depends on the annealing history. Annealing these samples at temperatures slightly below  $T_g$ , the strength of the secondary relaxation decreases and seems to vanish for long times [35]. In toluene on the other hand, this annealing effect could not be observed, neither in NMR- $T_1$  dispersion experiments nor with dielectric spectroscopy [36]. In

our simulations each small angle rotational jump leads to a new molecular orientation; no reorientations or librations around equilibrium positions were assumed. Therefore our small angle jumps differ from the dynamics typically assumed for secondary relaxation processes.

In a simple picture, different jump angles could also be explained assuming only one process. Then the large angle jumps ( $\sim 25^\circ$ ) are ascribed to elementary reorientations of the molecules. The large amount of small rotational jumps found in the experiment could be attributed to localized deformations, induced by the elementary jumps. If one molecule reorients by a  $25^\circ$  jump, the local potentials change and the neighboring molecules also will move, which could yield the small-angle contributions. In this context we note that an approach that takes the shoving work on the surrounding molecules into account was used to explain the temperature dependence of the viscosity in several supercooled liquids [37].

For a more detailed interpretation of the two-time correlation functions further data are required. Particularly systematic temperature dependent studies could give some hints as to the importance of a secondary process, since  $\alpha$  and slow  $\beta$  processes show significantly different temperature dependences. It should be noted that the data interpretation performed above ignores dynamical ‘‘exchange,’’ which is the subject of the following section.

### C. Dynamical heterogeneity

The stimulated echo experiment yielded two-time correlation functions, which decayed significantly nonexponentially. The reduced 4D NMR experiment allows one to elucidate this nonexponentiality further. In toluene- $d_5$  the transversal relaxation time  $T_2$  is very short ( $\sim 35 \mu\text{s}$ ) in the interesting temperature range above  $T_g$  and measuring the four-time correlation functions becomes very time consuming.

For the choice of an appropriate filter it is necessary to know the two-time rotational correlation function. We have measured  $F_2^{cc}(t_p, t_m)$  at  $T = 123$  K with an evolution time  $t_p = 30 \mu\text{s}$ . The choice of this value is the result of conflicting requirements. On the other hand,  $t_p$  should be large enough that any rotational jump will alter the NMR frequency so much that the jumped molecule will not contribute to  $F_2^{cc}$ . On the other hand  $T_2$  is the limiting factor to longer values, unfortunately. The problem of choosing a proper preparation time should be taken seriously, since otherwise not only dynamical exchange but also rotational dynamics contributes to the four-time correlation function [26].

The experimentally obtained two-time correlation function  $F_2^{cc}$  was fitted to  $\exp[-(t/\tau)^\beta]$  yielding the parameters  $\tau = 4.7 \times 10^{-4}$  s and  $\beta = 0.48$ . In analogy to previous experiments [11,13] the filter times  $t_m$  for the four-time correlation function were chosen to be on the same order as  $\tau$ . Figure 8 shows the four-time echo functions  $F_4$ , which were taken for two filter times  $t_m = 4.6 \times 10^{-4}$  s and  $7.8 \times 10^{-4}$  s, respectively. The decay of the  $F_4$  function signals that in toluene indeed slow subensembles could be selected. Since due to detailed balance after reequilibration ( $t_{m2} \rightarrow \infty$ ) some parts of the selected slow subensemble must remain slow, a finite plateau value is obtained.

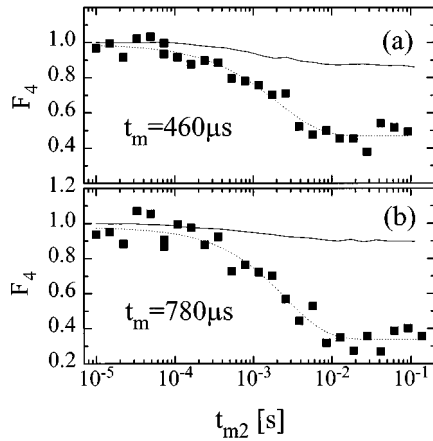


FIG. 8. Toluene- $d_5$  four-time rotational correlation functions  $F_4$  obtained with two different filter times  $t_m=460 \mu\text{s}$  (a) and  $t_m=780 \mu\text{s}$  (b), respectively. The solid lines result from simulations with the static correlation time distributions. The deviations demonstrate that this simplification does not hold, rather dynamical exchange has to be considered as being responsible for the decay of  $F_4$ .

To check the filter efficiency of the reduced 4D experiment, computer simulations as described above were performed. As input the rotational jump geometries of the two scenarios sketched in Fig. 7 were assumed. Orientational trajectories of single molecules were produced using the same algorithm as for the two-time rotational correlation functions (see Appendix A). No dynamical exchange was assumed in the calculations, which means that the rotational correlation time along one trajectory was constant. With the two angle model ( $4^\circ$  and  $25^\circ$ ) as well as with the distributed jump angle model the calculated  $F_4$  curves differ significantly from the experimental data (Fig. 8). This means that the simple static models used in the previous section cannot describe the experimental four-time correlation functions although they are sufficient for the two-time correlation.

In order to parametrize the  $F_4$  data we have used the Kohlrausch function

$$F_4(t_{m2}) = F_4^0 + (1 - F_4^0) \exp[-(t_{m2}/2\tau_{\text{ex}})^{\beta_{\text{ex}}}]$$

The results of the fits (Table I) show a significant dependence on the filter time  $t_m$ . With increasing  $t_m$  the decay time  $\tau_{\text{ex}}$  increases too. In addition, both correlation times  $\tau_{\text{ex}}$  and the corresponding reorientation time  $\tau$  from  $F_2^{cc}$  are of the same order of magnitude of time. This suggests that the time scales of reorientation and dynamical exchange are relatively similar.

We find a scenario that is comparable to that obtained previously in supercooled OTP [11]. There the four-time correlation functions could be described by using various mul-

TABLE I. Results for fits of the experimental  $F_4$  data to  $F_4(t_{m2}) = F_4^0 + (1 - F_4^0) \exp[-(t_{m2}/\tau_{\text{ex}})^{\beta_{\text{ex}}}]$ .

Filter	$\tau_{\text{ex}}$	$\beta_{\text{ex}}$	$F_4^0$
$t_m = 460 \mu\text{s}$	$2.0 \times 10^{-3} \text{ s}$	0.78	0.47
$t_m = 780 \mu\text{s}$	$2.6 \times 10^{-3} \text{ s}$	0.84	0.35

tistate rate exchange models. While these models deal with distributions of rotational and exchange rates, respectively, it was shown to be even sufficient to use only a single distribution of rates within the framework of an energy landscape model. Connecting the transitions from one energy minimum to another directly with a rotational jump process, experimental 4D data (OTP) could be well described [3]. In polymeric glass forming systems similar inhomogeneous scenarios were found previously [8,12,13], where the time scales of the selection and the reorientation are comparable.

With the reduced 4D experiment performed on toluene, we can identify inhomogeneous dynamics to be one reason for the nonexponentiality of two-time correlation functions. The return of selected subensembles occurs on the same time scale as the elementary jump process.

#### IV. SUMMARY

In this paper the rotational dynamics and geometry of toluene- $d_5$  is investigated in the supercooled state at temperatures slightly above  $T_g$ . Using multidimensional NMR techniques two- and four-time rotational correlation functions have been measured. Thus both the time scale and the geometry of the molecular reorientation are investigated at the same time. The temperature dependence of the measured NMR rotational correlation times is in accord with dielectric relaxation data [2], but the former are a factor of 10 slower. This cannot be explained by the different Legendre polynomials associated with the two methods.

While the rotational correlation times are accessible in the limit of vanishing evolution times  $t_p \rightarrow 0$  of the stimulated echo experiment, the rotational geometry is studied by measuring the explicit  $t_p$  dependence of the two-time correlation functions. Since the time window that is accessible with the NMR method is very narrow, the rotational geometry is studied only at one temperature  $T=122.2 \text{ K}$ . Data evaluation was performed by comparing experimental data with computer simulations of different rotational scenarios using a continuous time random walk algorithm. It is found that the assumption of only one jump angle does not describe the experimental data satisfactorily. Rather a distribution of jump angles is required. Already two different angles are sufficient to fit well to the experiment. The main contribution to molecular reorientation is due to small angle jumps  $<6^\circ$ , whereas more rarely larger jump angles up to  $30^\circ$  occur.

One property of correlation functions in supercooled liquids is the pronounced non-exponentiality. From other molecular glass forming systems like glycerol [10] and *o*-terphenyl [9,11] it is known that a heterogeneous scenario is at least partly responsible for the nonexponential decay of the two-time correlation functions. In toluene- $d_5$  we find a similar behavior at  $T=123 \text{ K}$ . Using a reduced 4D NMR experiment, slowly reorienting subensembles could be selected. It turns out that the residence times of molecules in the selected subensembles are on the same time scale as molecular reorientation.

#### ACKNOWLEDGMENTS

I wish to thank Roland Böhmer, Gregor Diezemann, Burkhard Geil, and Hans Sillescu for stimulating discus-

sions. This project was supported by the Deutsche Forschungsgemeinschaft Grant No. SFB#262, Project No. D9.

### APPENDIX A

We have used computer simulations to compare and interpret our experimental data. Basing on isotropic rotational jump processes, trajectories of individual molecules were recorded, which means that molecular orientations as a function of time were calculated. Once a trajectory is followed over a sufficiently long time interval, the different NMR pulse sequences can be applied. From the time dependent orientations the quadrupolar frequencies can be calculated directly. As a function of time only the reorientation of the molecules is considered when calculating the effect of the pulse sequences. Any further relaxation processes were neglected. In order to obtain the ensemble average  $\langle \dots \rangle$  in Eqs. (1)–(3), for one simulation typically more than  $10^6$  trajectories (molecules) were recorded. Care should be taken for the choice of the random number generator (we used ‘‘ran4’’ from [38]). To generate a trajectory, a continuous time random walk algorithm was used, which is outlined in the following:

(1) The starting orientation  $\Omega_i$  ( $i=1$ ) of one molecule is chosen randomly ensuring an isotropic distribution. The computer time  $t_i$  is set to zero. The first point of the trajectory is  $(t_1, \Omega_1)$ .

(2) The index  $i$  is incremented. The waiting time  $t_{wi}$  to the next event, which means a rotational jump, has to be determined. With the assumption of Poisson distributed jump events, the waiting times are chosen randomly from an exponential distribution [39]. The correlation time of the jump events is equal to the decay time of this distribution.

(3) A new orientation  $\Omega_i(\theta_i, \varphi_i)$  of the molecule has to be determined. This step depends on the jump model used in the simulation. If only one jump angle  $\Delta\theta$  should occur, then the new polar angle  $\theta_i$  with respect to the external magnet field is given by  $\theta_i = \arccos[\sin \theta_{i-1} \sin(\Delta\theta) \cos \psi + \cos \theta_{i-1} \cos(\Delta\theta)]$ , where  $\psi$  is chosen randomly between 0 and  $2\pi$ . If a distribution of jump angles is assumed, then for each rotational jump the jump angle  $\Delta\theta$  is determined randomly from the distribution. For the  $^2\text{H}$  NMR experiments performed in this work the azimuthal angles  $\varphi$  are irrelevant. With  $t_i$

$=t_{i-1}+t_{wi}$  the next point of the trajectory is  $(t_i, \Omega_i)$ .

(4) Steps (2) and (3) are repeated until the trajectory has reached the desired length, i.e.,  $t_i > t_{\max}$ .

### APPENDIX B

The calculation of a mean rotational jump angle depends on the correlation function considered, particularly on the rank  $L$  of that correlation function. Assuming only one rotational jump rate  $R_j = \tau_j^{-1}$  independent of the jump angle, the average jump angle can be calculated following Anderson [18]. For a single jump angle the *rotational* correlation function is given by

$$\Phi_L(t) = \exp\{-R_j t [1 + P_L(\cos \Delta\theta)]\} = \exp[-R_c t], \quad (\text{B1})$$

where  $P_L$  denotes the Legendre polynomial of order  $L$ . For  $L=2$  and  $R_c = \tau_c^{-1}$  Eq. (5) can be derived easily. If, for example, each rotational jump occurs with an angle chosen randomly from a bimodal distribution, i.e., from two jump angles  $\Delta\theta_1$  and  $\Delta\theta_2$  with probabilities  $p_1$  and  $p_2 = 1 - p_1$ , the resulting rotational correlation function can be written as

$$\Phi_L(t) = \exp\{-R_j p_1 t [1 + P_L(\cos \Delta\theta_1)]\} \exp\{-R_j p_2 t \times [1 + P_L(\cos \Delta\theta_2)]\}. \quad (\text{B2})$$

The generalization of Eq. (B2) to arbitrary distributions of jump angles is a straightforward task.

In this work the mean rotational jump angle  $\overline{\Delta\theta}$  is determined experimentally from the ratio of the jump and the rotational correlation times  $\tau_j/\tau_c$ , which now can be calculated for  $L=2$  with

$$\frac{\tau_j}{\tau_c} = \frac{3}{2} \sin^2 \overline{\Delta\theta} = \frac{3}{2} [p_1 \sin^2 \Delta\theta_1 + p_2 \sin^2 \Delta\theta_2]. \quad (\text{B3})$$

Equation (7) is the general expression for a continuous distribution of jump angles  $g(\Delta\theta)$ .

- 
- [1] F. Fujara, B. Geil, H. Sillescu, and G. Fleischer, *Z. Phys. B* **88**, 195 (1992).
- [2] A. Döb, G. Hinze, B. Schiener, J. Hemberger, R. Böhmer, *J. Chem. Phys.* **107**, 1740 (1997).
- [3] G. Diezemann, *J. Chem. Phys.* (to be published).
- [4] G. Diezemann, H. Sillescu, G. Hinze, and R. Böhmer, *Phys. Rev. E* (to be published).
- [5] W. Götze and L. Sjögren, *Rep. Prog. Phys.* **55**, 241 (1992).
- [6] R. Schilling and T. Scheidsteiger, *Phys. Rev. E* **56**, 2932 (1997).
- [7] P. Lunkenheimer, A. Pimenov, M. Dressel, Y. G. Gonsharov, R. Böhmer, and A. Loidl, *Phys. Rev. Lett.* **77**, 318 (1996).
- [8] K. Schmidt-Rohr and H. W. Spiess, *Phys. Rev. Lett.* **66**, 3020 (1991).
- [9] M. T. Cicerone and M. D. Ediger, *J. Chem. Phys.* **103**, 5684 (1995).
- [10] B. Schiener, R. Böhmer, A. Loidl, and R. V. Chamberlin, *Science* **274**, 752 (1996).
- [11] R. Böhmer, G. Hinze, G. Diezemann, B. Geil, and H. Sillescu, *Europhys. Lett.* **36**, 55 (1996).
- [12] J. Leisen, K. Schmidt-Rohr, and H. W. Spiess, *Physica A* **201**, 79 (1993).
- [13] A. Heuer, M. Wilhelm, H. Zimmermann, and H. W. Spiess, *Phys. Rev. Lett.* **75**, 2851 (1995).
- [14] G. Hinze, Ph.D. thesis 1993, University of Mainz.
- [15] G. Hinze and H. Sillescu, *J. Chem. Phys.* **104**, 314 (1996).
- [16] H. W. Spiess, *J. Chem. Phys.* **72**, 6755 (1980).
- [17] R. Böhmer and G. Hinze (unpublished).

- [18] J. E. Anderson, *Faraday Symp. Chem. Soc.* **6**, 82 (1972).
- [19] J. Wuttke, I. Chang, O. G. Randl, F. Fujara, and W. Petry, *Phys. Rev. E* **54**, 5364 (1996).
- [20] F. Fujara, S. Wefing, and H. W. Spiess, *J. Chem. Phys.* **84**, 4579 (1986).
- [21] K. Schmidt-Rohr and H. W. Spiess, *Multidimensional Solid-State NMR* (Academic Press, London, 1994).
- [22] B. Geil, F. Fujara, and H. Sillescu (unpublished); I. Chang, F. Fujara, B. Geil, G. Heuberger, T. Mangel, and H. Sillescu, *J. Non-Cryst. Solids* **172–174**, 248 (1994).
- [23] R. M. Diehl, F. Fujara, and H. Sillescu, *Europhys. Lett.* **13**, 257 (1990).
- [24] R. Böhmer, G. Diezemann, G. Hinze, and H. Sillescu, *J. Chem. Phys.* (to be published).
- [25] S. C. Kuebler, A. Heuer, and H. W. Spiess, *Phys. Rev. E* **56**, 741 (1997).
- [26] G. Hinze, R. Böhmer, G. Diezemann, and H. Sillescu (unpublished).
- [27] C. Alba, L. E. Busse, D. J. List, and C. A. Angell, *J. Chem. Phys.* **92**, 617 (1990).
- [28] R. Böhmer and C. A. Angell, in *Disorder Effects on Relaxation Processes*, edited by R. Richert and A. Blumen (Springer, Berlin, 1994), p. 11.
- [29] A. Kudlik, C. Tschirwitz, S. Benkhof, T. Blochowicz, and E. Rössler, *Europhys. Lett.* **40**, 649 (1997).
- [30] A. Heuer, J. Leisen, S. C. Kuebler, and H. W. Spiess, *J. Chem. Phys.* **105**, 7088 (1996).
- [31] L. J. Lewis and G. Wahnström, *J. Non-Cryst. Solids* **172–174**, 69 (1994).
- [32] M. Goldstein, *J. Chem. Phys.* **51**, 3728 (1969); G. P. Johari and M. Goldstein, *ibid.* **53**, 2372 (1970).
- [33] The methyl group rotation was studied in the glassy state and is much faster [14].
- [34] G. Hinze, H. Sillescu, and F. Fujara, *Chem. Phys. Lett.* **232**, 154 (1995).
- [35] C. Hansen and R. Richert (unpublished).
- [36] E. Rössler (private communication).
- [37] J. C. Dyre, N. B. Olsen, and T. Christensen, *Phys. Rev. B* **53**, 2171 (1996).
- [38] W. H. Press, S. A. Teukolsky, W. T. Vetterling, and B. P. Flannery, *Numerical Recipes in C* (Cambridge University Press, Cambridge, 1992).
- [39] N. G. van Kampen, *Stochastic Processes in Physics and Chemistry* (North-Holland, Amsterdam, 1981).